



Pull-out tests with CFRP laminates applied according to the ETS/NSM technique

C. A. N. da Silva ¹, J. Ciambella ¹, J. A. O. de Barros ² and I. G. Costa ³

¹ University of Rome Sapienza, Italy, Email : carlos.silva@uniroma1.it

² University of Minho, Portugal, ³ CiviTest, Portugal.

ABSTRACT

The retrofitting technique of Near-Surface Mounted (NSM) fiber-reinforced polymer (FRP) strips is receiving more attention recently due to many advantages over the externally bonded technique (EBR). However, in some situation is necessary to increase flexural and shear simultaneous. Therefore, to overcome this drawback, a hybrid strengthening technique that combines the advantages of NSM technique and Embedded Through Section (ETS) technique, is proposed by using an innovative CFRP laminate with rectangular shape in the NSM part and circular shape in the ETS. In order to evaluate the efficiency of the strengthening system, this paper presents the results of a series of pull-out tests using the innovative laminate to quantify the influence of the angle and embedded length. Using the results of this experimental program and developing a numerical strategy, an analytical bond stress–slip relationship was obtained.

KEYWORDS

CFRP - Strengthening – Direct Pullout - Bond - ETS - NSM - Laminate

INTRODUCTION

An effective method to increase the load-carrying capacity of existing reinforced concrete elements is by addition of tension reinforcement in surface grooves cut along the cover on the tension side (for flexural strengthening) or in the web (for shear strengthening) of these elements. A hybrid strengthening technique that combines the advantages of Near Surface Mounted (NSM) technique and Embedded Through Section (ETS) technique, is proposed by using an innovative CFRP laminate with rectangular shape in the NSM part and circular shape in the ETS. The L-shape laminate with an inclination angle aims to increase shear/punching resistance for RC beams/slabs, and anchorage the central part of the laminate, which provides flexural reinforcement to the RC elements. To evaluate the maximum tensile force, loaded-end slip, free-end slip and strain values of the innovative CFRP laminates with a L-shape configuration, direct pull-out tests were performed. Three embedment length values (Lb) for the CFRP laminates were analysed, 60, 120 and 180 mm, while for the inclination angle of the laminate extremity, three angles 15°, 30° and 45° as can be seen in Table 1. In order to evaluate the efficient of the strengthening system, pull-out test was carried by some authors (Coelho, Sena-Cruz and Neves, 2015; Cunha, 2010; Sena-Cruz, 2005) for understating the bond behaviour.

An analytical bond stress-slip relationship was determined for the innovative CFRP laminate. With this purpose, a numerical method was developed, which uses the results obtained in the experimental program. This method solves the differential equations that governs the slip evolution of the NSM/ETS CFRP laminate technique, and takes into account the distribution of the slip and the bond stress along the bond length. In the model was considered the variation of the tensile strain in the transition zone depth, due to the moment generated by the geometric curvature, and the embedded length as beam on elastic foundation. Using a numerical tool, the parameters that define the local bond stress-slip relationship and the friction between the materials are obtained. After demonstrating the good predictive performance of the proposed model, it shows the main conclusions and the future work.

Table 1 - Combination of the parameters analysed in the direct pull-out tests

<i>Direct pull-out test specimens</i>	Lb	CFRP laminate inclination angle (°)		
		15	30	45
CFRP laminate embedment length (Lb) (mm)	60	-	30-060	45-060
	120	-	30-120	45-120
	180	15-180	30-180	45-120

ANALYTICAL MODELLING

Bond between the innovative CFRP Laminate and Concrete (Pull-out Results)

The bond behaviour along the reinforcement was analysed as a uniaxial problem, and can be modelled by solving the differential equations that governs the behaviour of bond between the laminate and concrete. To solve these equations, the local bond stress-slip relationship must be known. In this section, an analytical bond stress-slip relationship was determined for the hybrid technique (NSM-ETS). Due to the non-linear local bond stress-slip relationship chosen, a numerical method was developed. This method solves the differential equations that governs the slip evolution of the innovative strengthening technique, and considers the variation of the tensile strain in the transition zone (TZO) depth, due to the moment generated by the geometric curvature. The embedded length (ETS) also has the contribution of shear force and bending moment. In the following sections this differential equation is deduced, the corresponding numerical method is detailed, and its performance is assessed.

Theoretical relationships for the local bond-slip

Assuming that CFRP has a linear-elastic behaviour, the equilibrium of a CFRP of length dx bonded to concrete can be given by the following expression:

$$\tau(s(x)) = \frac{A_f E_f}{p_f} \frac{d\varepsilon_f}{dx} \quad (1)$$

where A_f , E_f , σ_f , p_f and $\tau(s(x))$ is the cross-section area, Young's Modulus, normal strain, bond perimeter of the CFRP, and the local bond stress on the contact surface between the laminate and the concrete, respectively. In (Cruz and Barros, 2004; Cunha, Barros and Sena-Cruz, 2010; Kalupahana, 2009), the author have neglected the concrete and the adhesive deformability in the slip evaluation, because they claim the $\varepsilon_f \gg \varepsilon_c$. Therefore using the same assumption, the slip (s) is equal to the fiber displacement (u_f).

$$\frac{d^2 s}{dx^2} = \frac{d^2 u_f}{dx^2} \quad (2)$$

For a better representation of the innovative laminate behaviour, it was divided in 3 parts: NSM, TZO (transition zone) and ETS part. Each part has different mechanical properties, such as: modulus of elasticity, maximum tensile strength, cross section area and bond perimeter.

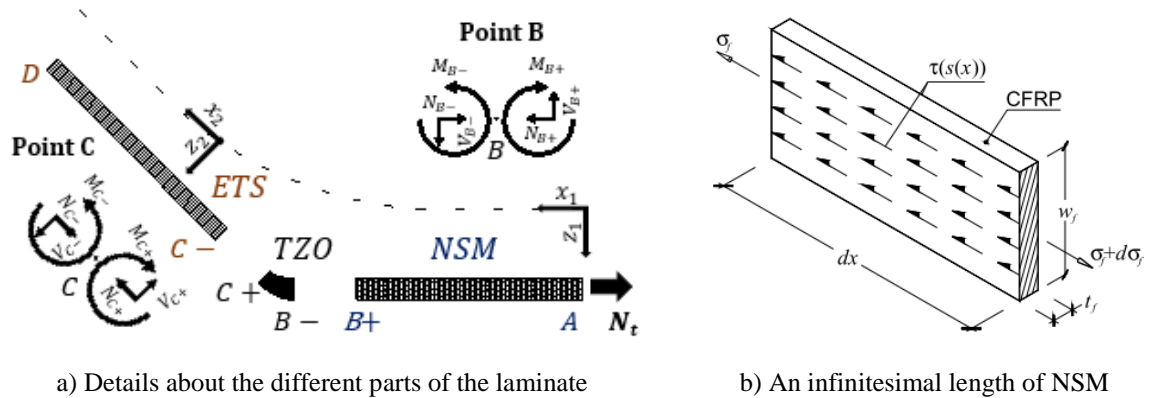


Figure 1 – Free body diagrams of the fiber

NSM

The deformation in NSM part is due to the axial force and its calculation can done as the variation of the slip/displacement in the normal direction. The differential equation that governs the slip of CFRP bonded into concrete is found:

$$\frac{d^2 s}{dx^2} = \frac{\tau(s) p_f}{A_f E_f} \quad (3)$$

To calculate the normal force was done by:

$$N_{NSM} = p_f \int_0^{L_{ef}} \tau(s(x)) dx \quad (4)$$

TZO

In the transition zone (TZO), the model considers the addition strain caused by the bending moment (Eq. 5). This moment is generated due to the curvature according to Timoshenko curved beam theory (Timoshenko, 1955).

$$\varepsilon = \frac{1}{(1+z/R)} \left(\frac{du_f}{dx} + \frac{w}{R} + z \frac{d\theta}{dx} \right) \quad (5)$$

Using the beam curvature equation together with the equations of equilibrium for a curved element:

$$\frac{d^2w}{dx^2} = \frac{M}{EI} \quad \frac{dN}{dx} = \tau(s)p_f \quad \frac{dN}{dx} + \frac{V}{R} = 0 \quad \frac{dM}{dx} - V = 0 \quad \frac{d^3w}{dx^3} = \frac{-\tau(s)p_f R}{E_f I_f} \quad (6)$$

Results in the fundamental governing ordinary differential equation for the transition part (TZO):

$$\frac{d^4s}{dx^4} = \frac{pf}{AfE_f} \left(1 + \frac{z}{R} + \frac{zRAf}{I_f} \right) \left(pf \frac{d^2\tau(s)}{dx^2} \left(\frac{ds}{dx} \right)^2 + \frac{d\tau(s)}{ds} \frac{d^2s}{dx^2} \right) + \frac{pf}{I_f E_f} \tau(s) \quad (7)$$

where w , R , θ , z and I_f denote the normal deflection, the radius of curvature, the rotation, the thickness coordinate measured from the centreline and the moment of inertia respectively. The force in the TZO is calculated as in NSM part, the integral of the slip function over the length.

ETS

For the embedded part of the fiber was modelled as a beam on elastic foundation, the deflection (w) is a function of the local coordinate x along the fiber satisfying the following governing equation:

$$EI \frac{d^4w}{dx^4} + Kw = 0 \quad \text{with} \quad K = \frac{2E_c(1-\nu_c)}{(1+\nu_c)(1-2\nu_c)\ln(t/\phi)} \quad (8)$$

where E_c and ν_c are the Young's modulus and Poisson's ratio of the concrete matrix, t is the thickness of the matrix around the fiber and ϕ is the diameter. The deflection is given by:

$$w(x) = e^{\beta x} (C_1 \sin \beta x + C_2 \cos \beta x) + e^{-\beta x} (C_3 \sin \beta x + C_4 \cos \beta x) \quad (9)$$

where $\beta = (K/4EI)^{1/4}$. The constants ($C_1 - C_4$) are found by imposed the following boundary conditions:

$M(L_{ef}^i) = 0$, $M(L_{ETS}) = M_C$, $V(L_{ef}^i) = 0$ and $V(L_{ETS}) = V_C$. The effective length (L_{ef}^i) will be explained in the

description of the method (1^o step). Therefore, the distributed reaction force of the foundation is: $F(x) = -Kw(x)$.

A reduction of the foundation reaction (F') and the modified frictional (ξ) along the branch was considered by means of an empirical formula (Zhan and Meschke, 2014):

$$F'(x) = \begin{cases} |F(x)| & \text{if } \eta \leq 1 \\ \phi_{ck} (\ln^2 \eta + 1) & \text{if } \eta > 1 \end{cases} \quad \xi(s) = \xi_0 + \xi_p = \begin{cases} (1-\eta/2)p_f\tau(s) + \mu F'(x) & \text{if } \eta \leq 1 \\ p_f\tau(s)/2 + \mu F'(x) & \text{if } \eta > 1 \end{cases} \quad (10)$$

where $\eta = |F(x)| / (\phi_{ck})$ indicates the degree of utilization of the foundation compressive strength, ξ_0 indicates the remaining portion of the pure frictional stress and ξ_p additional Coulomb's friction resulting from the deflection of the fiber and μ is the friction coefficient. With these assumptions, the pull force for the ETS part is:

$$N_{ETS} = \int_{L_{AC}}^{L_{ef}} \xi(s(x)) dx \quad (11)$$

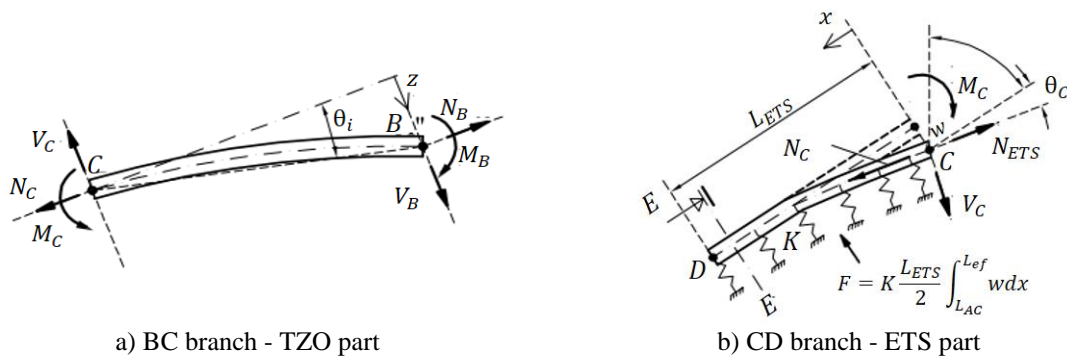


Figure 2 – Free body diagrams of the inclined region

Local Bond Stress-Slip Relationship

Analytical expressions for the local bond stress-slip relationship

For characterizing the local bond stress-slip relationship was chosen the following exponential functions:

$$\tau(s) = \begin{cases} \tau_m (s / s_m)^g & \text{if } s \leq s_m \\ \tau_m (s / s_m)^{-g'} & \text{if } s > s_m \end{cases} \quad (12)$$

where τ_m is the bond strength, s_m is the slip where occurs the maximum stress, g and g' are the parameters that define the curves shape, the ascending and descending branch respectively.

Boundary Conditions

The governing equations can now be solved by using the relationship for the interface shear-stress/slip characteristic, along with the boundary conditions. The boundary conditions in points A, B, C and D are:

$$x = A \rightarrow \begin{cases} s_A = s_{load} \\ N_A = N_t \\ \varepsilon_A = \frac{N_A}{E_f A_f} \end{cases} \quad x = B \rightarrow \begin{cases} s_{B-} = s_{B+} \\ N_{B-} = N_{B+} \\ n_N^T \varepsilon_{B-} = \varepsilon_{B+} \\ n_N^T \varepsilon'_{B-} = \varepsilon'_{B+} \end{cases} \quad x = C \rightarrow \begin{cases} s_{C-} = s_{C+} \\ N_{C-} = N_{C+} \\ n_T^E \varepsilon_{C-} = \varepsilon_{C+} \\ n_T^E \varepsilon'_{C-} = \varepsilon'_{C+} \end{cases} \quad x = D \rightarrow \begin{cases} s_D = \bar{s} \text{ free} \\ N_D = 0 \\ \varepsilon_D = 0 \end{cases} \quad (13)$$

being B- and B+ the values of point B slightly left and right respectively, see Figure 1 a). The constants (n_N^T, n_T^E) were found by doing the equilibrium force in points B and C:

$$n_N^T = \frac{E_{B-} A_{B-}}{E_{B+} A_{B+}} = \frac{E_f^{TZO} A_f^{TZO}}{E_f^{NSM} A_f^{NSM}} \quad n_T^E = \frac{E_{C-} A_{C-}}{E_{C+} A_{C+}} = \frac{E_f^{ETS} A_f^{ETS}}{E_f^{TZO} A_f^{TZO}} \quad (14)$$

NSM/ETS

The initial guess solve the second order differential equation (Eq. 3) are the slip (s) and the its first derivate (s'). In all step the first derivate is equal to zero ($s'(x = L_{ef}^i) = 0$), concerning the slip (s) it was divided in two possibilities: 1° to 3° steps - $L_{ef}^i < L_t \rightarrow s(x = L_{ef}^i) = 0$; 4° step - $L_{ef}^i = L_t \rightarrow s(x = L_t) = \bar{s}_{free}$. Where L_{ef}^i is the effective length, that will be presented in the description of the method.

TZO

The input to solve the 4 order differential equation (Eq.7) are the slip (s), the first, second and the third derivative (s', s'', s'''). In order to maintain the continuity of the slip function in the ETS part, it was fitted with a 4-order polynomial function. At the transition (point C), the value of this fuction was calculated ($d0, d1, d2$ and $d3$) and were assumed as input to the TZO part (Table 2). The full description is explained in next subsection.

Table 2 - The input to solve the 4 order differential equation for the TZO part

Step	Part	Point	$s(x)$	$s'(x)$	$s''(x)$	$s'''(x)$
2°	TZO	$x = L_{ef}^i$	0	0	0	0
	NSM	$x = B+$	s_{B-}	$n_N^T s_{B-}$	-	-
3° and 4°	TZO	$x = C+$	$d0$	$n_T^E d1$	$n_T^E d2$	$d3$
	NSM	$x = B+$	s_{B-}	$n_N^T s_{B-}$	-	-

Description of the method

As described in (Cunha, Barros and Sena-Cruz, 2010) the present method, both numerical and experimental entities are simultaneously compared, hence the experimental ones were distinguished by an overline, i.e. \bar{N}^i , stands for the pull-out force experimentally measured in the i-th scan read-out. The pull-out tests provide the load, \bar{N}^i , the free and load end slip (\bar{s}^i_{free} and \bar{s}^i_{load}). Using these experimental results, the set of unknown parameters of a given local bond relationship is obtained by fitting the differential equations 3 and 7 as accurately as possible. A computational code was developed in Matlab® software, supported on the algorithm showed in

Figure 3. The differential equations included in the algorithm are solved by the Runge-Kutta-Nystrom (RKN) method (Kreyszig, Erwin and Norminton, 1993). The algorithm is built up from the following main steps:

The first initial guess for the unknown parameters ($\tau-s$ relationship and μ) is defined.

1^o step - Developing the NSM branch (L_{NSM})

The loaded end slip (s_{load}^i) is calculated with the initial guess $s(L_x^j) = s'(L_x^j) = 0$. The s_{load}^i calculated is compared with the i-th scan reading (\bar{s}_{load}^i). If the calculate value is smaller than the experimental, it means the effective length (L_{ef}^i) is higher than the initial length $L_x^j < L_{ef}^i < L_{NSM}$ (See Module A). The L_{ef}^i is calculated interactively ($L_x^j = L_x^j + \delta$) until $s_{load}^i \cong \bar{s}_{load}^i$. This interactively procedure is repeated in 1^o - 3^o steps, until the total laminate length is mobilized. Therefore, the determination of the total force N_t^i is with the L_{ef}^i . When the value $L_{ef}^i \geq L_{NSM}$ starts to develop the contribution of the transition zone (TZO).

2^o step - Developing the TZO branch (L_{TZO})

In this step was used Modules B and C. The input are: $s_0 = s' = s'' = s''' = 0$ and L_x^j . The compatibility between the TZO and NSM part is done by: $s_{B+} = s_{B-}$ and $\varepsilon_{B+} = n_N^T \varepsilon_{B-}$. The effective length is calculated as in 1^o step. When L_{ef}^i reaches $L_{NSM} + L_{TZO}$, its starts to add the contribution of the ETS part and $N_t^i = N_{TZO}^i + N_{NSM}^i$.

3^o step - Developing the ETS branch (anchorage)

Using the values of the bending moment and the shear force in C (M_C, V_C) for the previous step together with L_x^j is determined the initial deflection (w). Therefore, it is evaluated the foundation reaction and the modified frictional is obtained (See Module D). The loaded end slip is calculated using Modules E, F and C with the initial guess $s_0 = s' = 0$. The compatibility between the ETS and TZO part is done by as follows: $s_{D+} = d_0$, $\varepsilon_{D+} = n_T^E d_1$, $\varepsilon_{D+} = n_T^E d_2$ and d_3 . The values, (d_0, d_1, d_2 and d_3) were presented in the boundary conditions section. The effective length is calculated as in 1^o step and the compatibility in point B was done as in the 2^o step. The total force is: $N_t^i = N_{NSM}^i + N_{TZO}^i + N_{ETS}^i$.

4^o step - Increasing the free end slip

The total laminate length has been already mobilized, thus, it is not necessary to performed the interactively procedure done in 1^o - 3^o steps. In this step, the effective length (L_{ef}^i) is equal to the total length ($L_{ef}^i = L_t$). However, using Module D is calculated the initial deflection, foundation reaction and the modified frictional because the bending moment and shear force in point C change in each interaction. Therefore, taking the free end slip from the experimental data, the numerical pull-out force at the loaded end is calculated.

5^o step

The maximum force error ($e^f = (N_{max} - \bar{N}_{max})/\bar{N}_{max}$) and the slip error where the maximum force occurs ($e^s = (s_m - \bar{s}_m)/\bar{s}_m$) are calculated.

To use it for the hybrid technique (NSM-ETS) several issues must be clarified. The pull-out behaviour of the fiber is a very complex problem, since several mechanisms interact with each other's during pull-out. Therefore, to simulate inclined part the following aspects were neglected: the mechanical properties of the resin, spalling of the concrete matrix at the fiber exit point and the imperfections in the transition zone as in (Cunha, Barros and Sena-Cruz, 2010). The determination of the unknown parameters defining the bond stress - relationship ($\tau-s$ and μ), was performed by a back-analysis, i.e. determining theses values in such a way that to the peak pull-out load and its corresponding slip are close to the values experimentally measured. The back-analysis was performed by brute force method as described in (Cruz and Barros, 2004) based on several parameters sets ascertained by a predefined range and step for each parameter of the corresponding set.

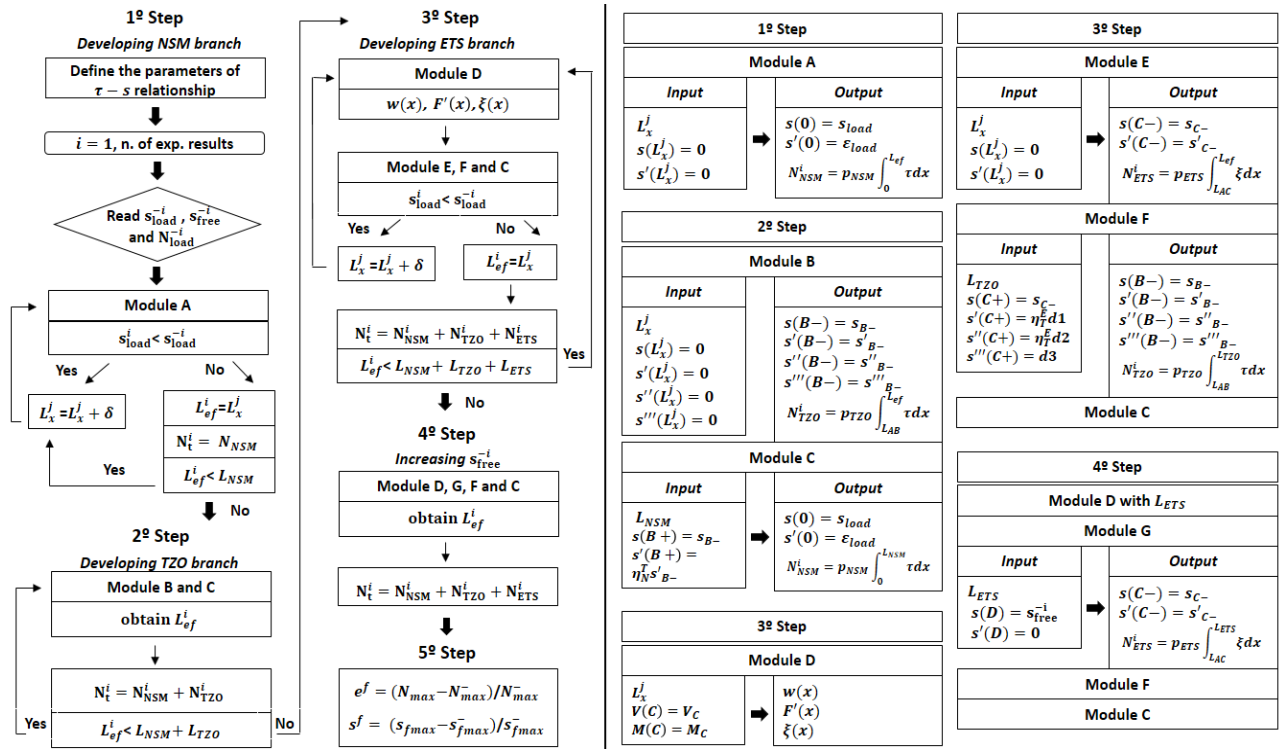


Figure 3 – Implemented algorithm to obtain the local bond-stress slip relationship

EXPERIMENTAL PROGRAM

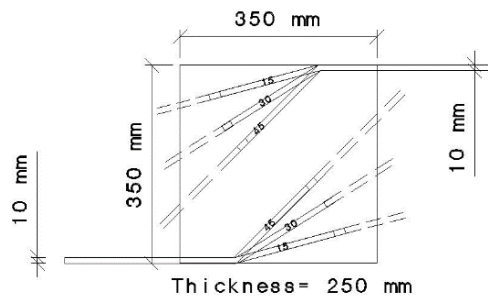
Material properties

Table 2 - Mechanical properties of the materials

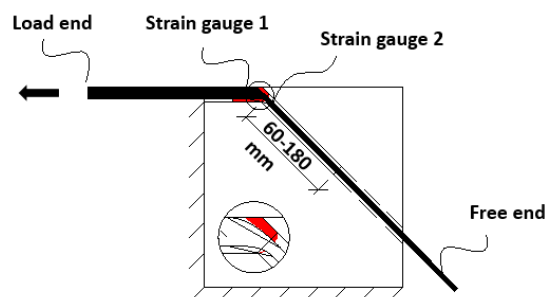
Material	Compression Stress (MPa)	Tensile Stress (MPa)	Elastic Modulus (MPa)
Concrete	25	1.9	24500
CFRP	-	2000	155000
S&P 220 Resin	>70	20	7420
S&P 55 Resin	-	35	2585

Configuration

In Figure 4a) is shown the difference between the angles analyzed and 4b) are presented the location of the strain gauges in the beginning/end of the transition zone.



b) Difference between the angles studied



a) Location of the strain gauges in the laminates

Figure 4 – Details about the configurations

Test Setup

The test setup defined to perform the direct pull-out test is presented in Figure 5.

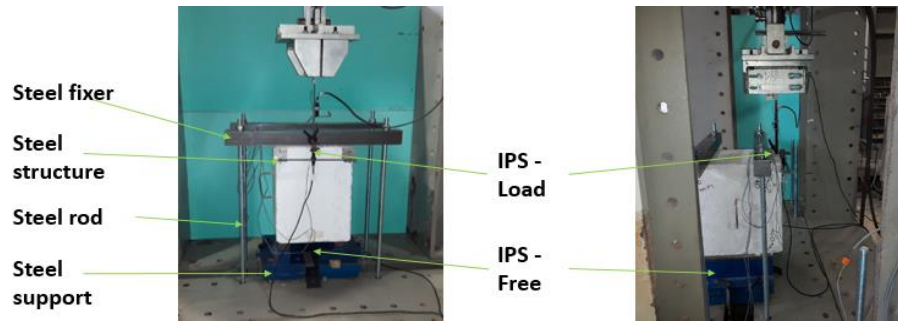


Figure 5 – Test Setup - Front and Lateral views

Failure Mode

The observed failure mode for all the experimental push–pull tests is fiber rupture in beginning of the transition zone.

RESULTS AND DISCUSSIONS

As can be seen in Figs. 6 and 7, the analytical model provides good accuracy with the experimental results for the innovative laminate. Since all laminates had the same failure mode, was confirmed that the critical region is the transition zone. The maximum deformation recorded by strain gauge 1 has provided a criterion for stopping the algorithm. These values of strains at beginning (Point B) and end (Point C) of TZO was compared with experimental measured by the strain gauges installed in the laminate (Fig. 7). The analytical model could not predict well the results for the deformations in the transition zone at the beginning of loading. This is due to the NSM part needs to be fully mobilized so it starts to developed the transition zone. In the experiments carried out, due to premature rupture of the transition zone, the entire length of the laminate was not mobilized. Thus, in these cases it was not necessary to use the free end slip values.

Table 3 - Values of the parameters defining the local bond stress-slip relationship

Serie	s_m [mm]	τ_m [MPa]	ϑ	ϑ'	μ	e^f [%]	e^s [%]
fc25_a15_Lb180	0.15	25.5	0.47	0.71	0.30	0.75	0.92
fc25_a30_Lb120	0.17	28.4	0.59	0.75	0.30	1.19	0.85

The unknown parameters of the local bond relationship for the specimen fc25-a15-Lb180 and fc25-a30-Lb120 are showed in 3. The laminate with a 15° inclination angle has achieved a pull-out force of 21,3 kN (Fig. 6 a), and the 30° of 20,7 kN (Fig. 6 b). According to the manufacture of the laminates used, the maximum tensile force expected for conventional laminates is 28 kN (particularly, a maximum tensile force of 2000 MPa and an elasticity modulus of 155 GPa). Therefore, the maximum force achieved is 75 % of the full capacity of the CFRP laminate. The slip value at the maximum force was 0.37 mm for 15° and 0.42 mm for 30°. In the beginning of the transition zone, the laminates with 15° and 30° achieved the maximum tensile strain value of 5,21 ‰ and 6,73 ‰ at maximum force, i.e., 39,17 % and 50,60 % of the tensile strain value expected for the laminate used. After the transition zone, the laminates with 15° and 30° reach the tensile strain value that corresponds to 0,28 ‰ and 0,39 ‰, that is 2,10 % and 2,93 % of the expected maximum tensile strain value.

CONCLUSIONS

A research was developed to calibrate the parameters that define a local bond stress–slip relationship able to reproduce the pre- and the post- peak bond stress phases of the bonding between concrete and laminate of carbon fiber reinforced polymer (CFRP) in NSM/ETS strengthening technique. The research involved data obtained in experimental tests and a numerical strategy developed to solve two differential equations that governs the slip phenomenon. Due to the limitations on the experimental test facilities, the deformability of the epoxy adhesive, the CFRP-adhesive slip and the adhesive-concrete slip could not be measured, resulting in a local bond stress-slip relationship which is dependent on the bond length. Besides of a different resin was used in the ETS part, for reasons of simplification, the same local bond stress-slip relationship adopted for the entire laminate. The results revealed that all laminates had almost the same maximum force, due to the same premature failure, in the beginning of their transition zone. The next activities will be improving the fiber in the transition zone, avoiding

the premature failure and reaching the maximum potential of tensile strength. Then, it will be possible to confirm the validity of the proposed analytical model.

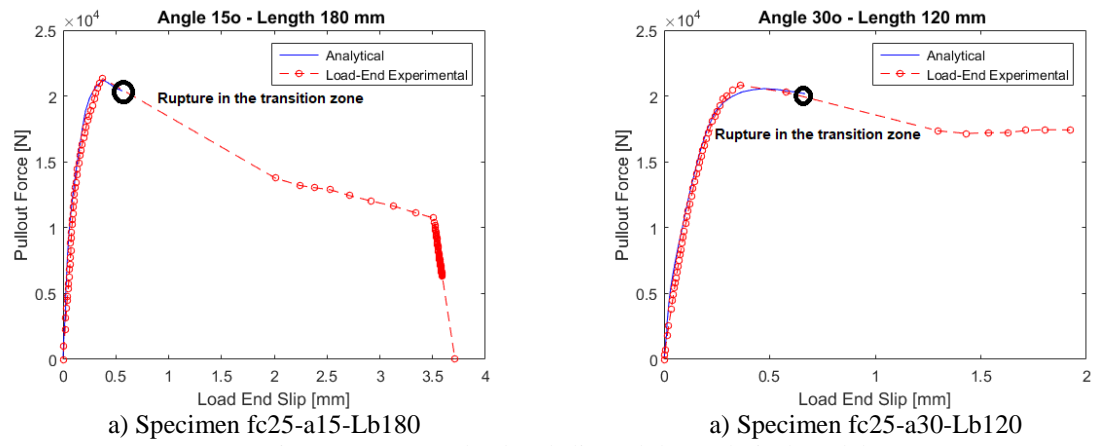


Figure 6 – Force - load end slip and the analytical model

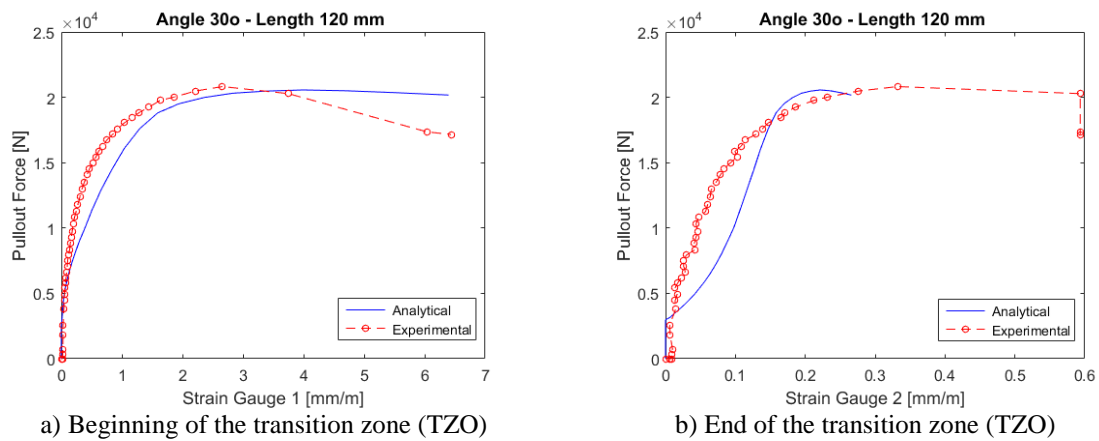


Figure 7 – Experimental strain and the analytical values for the specimen fc25-a30-Lb120

ACKNOWLEDGMENTS

The authors of the present work wish to acknowledge the supports provided by the S&P®.

REFERENCES

- Coelho, M.R.F., Sena-Cruz, J.M. and Neves, L.A.C., 2015. A review on the bond behavior of FRP NSM systems in concrete. *Construction and Building Materials*, 93, pp.1157–1169.
- Cruz, J.S. and Barros, J.A.O., 2004. Modeling of bond between near-surface mounted CFRP laminate strips and concrete. *Computers and Structures*, 82(17–19), pp.1513–1521.
- Cunha, V.M.C.F., 2010. *Steel fibre reinforced self-compacting concrete (from micromechanics to composite behavior)*.
- Cunha, V.M.C.F., Barros, J.A.O. and Sena-Cruz, J.M., 2010. Pullout Behavior of Steel Fibers in Self-Compacting Concrete. *Journal of Materials in Civil Engineering*, 22(1), pp.1–9.
- Kalupahana, W.K.K.G., 2009. Anchorage and Bond Behaviour of Near Surface Mounted Fibre Reinforced Polymer Bars. *Department of Architecture and Civil Engineering*, PhD.
- Kreyszig, Erwin and Norminton, E.J., 1993. *Maple computer manual for advanced engineering mathematics*. John Wiley & Sons, Inc.
- Sena-Cruz, J.M., 2005. *Strengthening of concrete structures with near-surface mounted CFRP laminate strips*. PhD Thesis.
- Timoshenko, S., 1955. *Strength of Materials-part I Elementary Theory and Problems*. D. Van Nostrand Co., Princeton, NJ.
- Zhan, Y. and Meschke, G., 2014. Analytical Model for the Pullout Behavior of Straight and Hooked-End Steel Fibers. *Journal of Engineering Mechanics*, 140(12), p.4014091.